

SPECTRAL PRECONDITIONERS FOR NONHYDROSTATIC ATMOSPHERIC MODELS: EXTREME APPLICATIONS

P.K. Smolarkiewicz*, C. Temperton†, S.J. Thomas*, A.A. Wyszogrodzki‡

*National Center for Atmospheric Research, Boulder, Colorado, U.S.A.

† European Centre for Medium Range Weather Forecasts, Reading, UK.

‡ Los Alamos National Laboratory, Los Alamos, New Mexico, U.S.A.

Motivation

- We are concerned with DNS/LES of high Reynolds number and low Mach number flows — i.e., highly turbulent and essentially incompressible flows — of inhomogeneous anisotropic fluids with restoring forces, viz. *complex fluids*.
- The associated elliptic BVPs are poorly conditioned ($\kappa \sim \mathcal{O}(10^{10})$ for terrestrial GCMs) nonseparable, containing cross derivatives, and nonsymmetric — due to domain anisotropy, planetary rotation, stratification, curvilinear coordinates, irregular lower boundary, etc.
- Such BVPs are difficult — i.e., a universally-effective solution does not exist. Each particular case may call for a user's intervention in customizing the elliptic solver, to achieve a judicious compromise between the accuracy and computational expense.

Approach

- An introduction to CG methods (from PDE perspective): Smolarkiewicz & Margolin. Variational methods for elliptic problems in fluid models. *Proc. ECMWF Workshop on Developments in numerical methods for very high resolution global models* 5-7 June 2000; Reading, UK, ECMWF, 137–159.

- Our method of choice is the restarted generalized conjugate residual GCR(k) algorithm (Eisenstat et al., 1983, *SIAM J. Numer. Anal.*) proven successful in geophysical applications.

- An artful *preconditioner* can dramatically accelerate solver convergence!

- We consider spectral methods in the horizontal, with a line-relaxation scheme in the vertical.

Continuity of Efforts

- Bernardet (1995, MWR); Elman & O’Leary (1998, JCP)
- Thomas et al. (2003, MWR) reported advantages of spectral preconditioning, in the context of the serial code of the Canadian MC2 model — a semi-Lagrangian, semi-implicit elastic, nonhydrostatic all-scale research/weather-prediction type model.
- We continue in the context of the massively-parallel, nonhydrostatic anelastic, deformable-grid, Eulerian/semi-Lagrangian model EULAG for multi-scale research of geophysical flows.

Preconditioned GCR(k) Scheme, for $\mathcal{L}(\phi) - R = 0, \mathcal{P} \approx \mathcal{L}$

$$\frac{\partial^k \mathcal{P}(\phi)}{\partial \tau^k} + \frac{1}{T_{k-1}} \frac{\partial^{k-1} \mathcal{P}(\phi)}{\partial \tau^{k-1}} + \dots + \frac{1}{T_1} \frac{\partial \mathcal{P}(\phi)}{\partial \tau} = \mathcal{L}(\phi) - R \implies$$

For any initial guess Ψ_i^0 , set $r_i^0 = \mathcal{L}_i(\Psi^0) - Q_i$, $p_i^0 = \mathcal{P}_i^{-1}(r^0)$; then iterate:

For $n = 1, 2, \dots$ until convergence do

for $\nu = 0, \dots, k-1$ do

$$\beta = -\frac{\langle r^\nu \mathcal{L}(p^\nu) \rangle}{\langle \mathcal{L}(p^\nu) \mathcal{L}(p^\nu) \rangle},$$

$$\Psi_i^{\nu+1} = \Psi_i^\nu + \beta p_i^\nu, \quad r_i^{\nu+1} = r_i^\nu + \beta \mathcal{L}_i(p^\nu),$$

exit if $\| r^{\nu+1} \| \leq \varepsilon$,

$$e_i = \mathcal{P}_i^{-1}(r^{\nu+1}),$$

$$\mathcal{L}_i(e) = \left[\sum_{I=1}^M \frac{\partial}{\partial x^I} \left(\sum_{J=1}^M C^{IJ} \frac{\partial e}{\partial x^J} + D^I e \right) - A e \right]_i,$$

$$\forall_{l=0, \nu} \alpha_l = -\frac{\langle \mathcal{L}(e) \mathcal{L}(p^l) \rangle}{\langle \mathcal{L}(p^l) \mathcal{L}(p^l) \rangle},$$

$$p_i^{\nu+1} = e_i + \sum_{l=0}^{\nu} \alpha_l p_i^l, \quad \mathcal{L}_i(p^{\nu+1}) = \mathcal{L}_i(e) + \sum_{l=0}^{\nu} \alpha_l \mathcal{L}_i(p^l),$$

end do,

reset $[\Psi, r, p, \mathcal{L}(p)]_i^k$ to $[\Psi, r, p, \mathcal{L}(p)]_i^0$,

end do.

assuming $\forall_\xi \langle \xi \mathcal{L}(\xi) \rangle \leq 0$, with “=” holding if and only if $\langle \xi \xi \rangle = 0$.

Line-relaxation Preconditioners

• Anisotropy in the vertical $L_z/L_h \ll 1 \implies$ simple, yet effective preconditioners, derivable from the Richardson (1910, Phil. Trans. Roy. Soc.) scheme:

$$\frac{e^{\mu+1} - e^\mu}{\delta\tilde{\tau}} = \mathcal{P}^h(e^\mu) + \mathcal{P}^z(e^{\mu+1}) - r^{\nu+1}, \quad \mathcal{P} \equiv \mathcal{L} - CDT, \quad (1)$$

where, \mathcal{P}^h and \mathcal{P}^z are the horizontal and the vertical counterparts of \mathcal{P} , $\delta\tilde{\tau}$ is the iteration parameter (based on spectral properties of \mathcal{P}^h), μ numbers successive Richardson iterations, ν numbers the outer iterations of GCR(k), and CDT denotes cross-derivative terms.

• Eq.(1) leads to a linear problem

$$(\mathcal{I} - \delta\tilde{\tau}\mathcal{P}^z)e^{\mu+1} = \tilde{R}^\mu, \quad \tilde{R}^\mu \equiv e^\mu + \delta\tilde{\tau}(\mathcal{P}^h(e^\mu) - r^{\nu+1}), \quad (2)$$

readily invertible using a Thomas' algorithm; alternating implicit discretization between \mathcal{P}^h and \mathcal{P}^z in fractional steps of $\tilde{\tau}$ leads to alternating-direction-implicit (ADI) preconditioners (Skamarock et al., MWR, 1997).

• The preconditioner in (1) can be improved ($\sim 10\%$) by extending the scheme to the diagonally-preconditioned Duffort-Frankel algorithm

$$\frac{\mathcal{D}e^{\mu+1} - \mathcal{D}e^\mu}{\delta\tilde{\tau}} = \mathcal{P}^h(e^\mu) - \mathcal{D}(e^{\mu+1} - e^\mu) + \mathcal{P}^z(e^{\mu+1}) - r^{\nu+1}, \quad (3)$$

where $(-1)\mathcal{D}$ stands for the diagonal coefficient embedded within the matrix representing \mathcal{P}^h on the grid. As $\delta\tilde{\tau} \rightarrow \infty$, (3) \rightarrow block Jacobi preconditioner.

Spectral Preconditioning

• The idea is to allow for the “ μ -implicitness” in the horizontal, and to converge with $\delta\tilde{\tau} \rightarrow \infty$ in the Richardson iteration, so

$$\begin{aligned} \frac{e^{\mu+1} - e^\mu}{\delta\tilde{\tau}} &= \mathcal{P}^h(e^\mu) + \mathcal{P}^z(e^{\mu+1}) - r^{\nu+1} \implies \\ &\mathcal{P}^h(e^{\nu+1}) + \mathcal{P}^z(e^{\nu+1}) = r^{\nu+1} \end{aligned} \quad (4)$$

becomes iteration free.

• Assuming $e^{\nu+1} = \sum_{k,l} \hat{e}_{k,l}(z) \exp[i(k \cdot x + l \cdot y)]$, and same for $r^{\nu+1}$, leads to

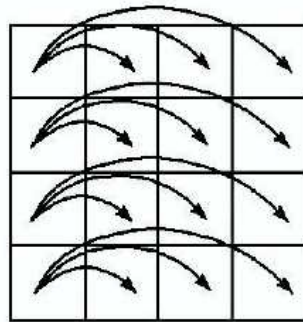
$$\sum_{k,l} \{ \mathcal{C}_{k,l}(z) \hat{e}_{k,l} + \mathcal{B}_{k,l}(z) \frac{d^2 \hat{e}_{k,l}}{dz^2} - \hat{r}_{k,l} \} \exp[i(k \cdot x + l \cdot y)] \equiv 0, \quad (5)$$

and to the corresponding set of independent linear tridiagonal problems in the Fourier space,

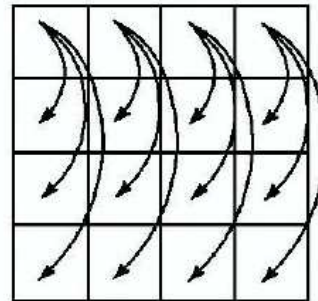
$$\forall_{k,l} \quad \left(\mathcal{C}_{k,l}(z) + \mathcal{B}_{k,l}(z) \frac{\delta^2}{\delta z^2} \right) \hat{e}_{k,l}(z) = \hat{r}_{k,l}(z) \quad (6)$$

- ISSUES: i) *coefficient homogenization* within \mathcal{P} — to avoid Fourier transforms of the coefficients themselves, and multiplying the resulting series; ii) *massively-parallel* implementations.

- APPROACH: custom-programmed tensor-product 2D Fourier transformations (for either periodic or open boundaries) with a fully-distributed spectral space, in the spirit of the domain-decomposition employed for the physical space.



distributed 1D FFT



distributed 1D FFT

Figure 1: Static block distribution (SBD) method for computing tensor-product Fourier transforms, Calvin (1996, Parall. Comp.), becomes static local (SLD) as processors array \rightarrow 1D

Anelastic Model: Analytic Formulation

○ Prusa & S., *JCP* 2003; Wedi & S., *JCP* 2004; Prusa & S. *ibid.*

● (physical domain) $\mathbf{S}_p \rightarrow \mathbf{S}_t$ (computational domain)

$$(\bar{t}, \bar{\mathbf{x}}) \equiv (t, \mathcal{F}(t, \mathbf{x})) \quad (7)$$

● Assumptions:

- 1) \mathbf{S}_p and \mathbf{S}_t are (topologically) cuboidal, toroidal, or spheroidal;
- 2) coordinates (t, \mathbf{x}) of \mathbf{S}_p are orthogonal and stationary;
- 3) $\bar{t} \equiv t$;
- 4) (\bar{x}, \bar{y}) are independent of z .
- 5) (7) is a *diffeomorphic* mapping (*homeomorphism* OK)

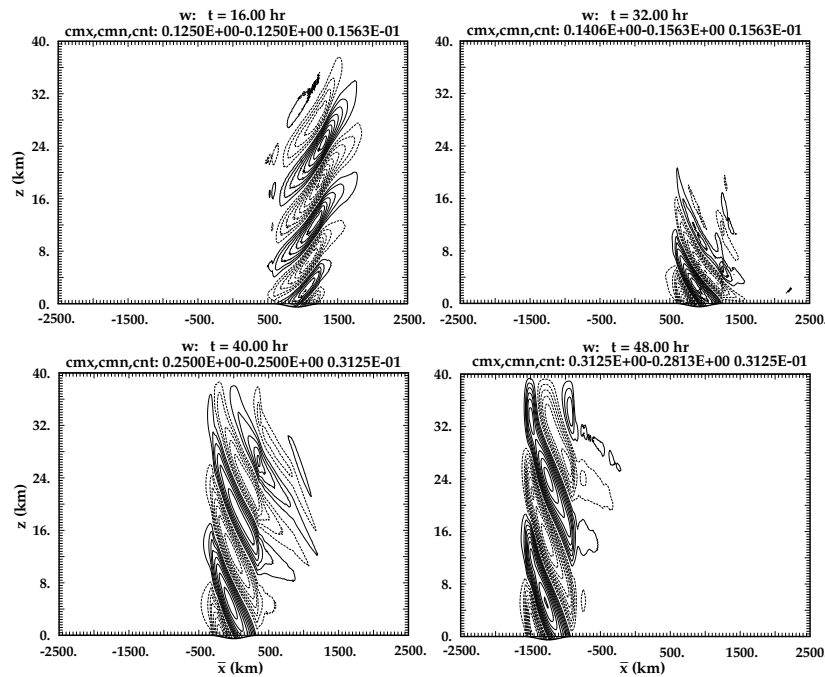


Figure 2: Gravity-wave packet past oscillating source.

- Anelastic system of Lipps & Hemler (*J. Atmos. Sci.*, 1982)

$$\bar{\nabla} \bullet (\rho_b \bar{G} \bar{\mathbf{v}}^s) = 0 . \quad (8)$$

$$\frac{d\mathbf{v}}{dt} = - \tilde{\mathbf{G}}(\bar{\nabla}\pi') - \mathbf{g} \frac{\theta'}{\theta_b} - \mathbf{f} \times \mathbf{v}' + \mathbf{M}' + \mathbf{D} , \quad (9)$$

$$\frac{d\theta'}{dt} = -\bar{\mathbf{v}}^s \bullet \bar{\nabla}\theta_e + \mathcal{H} , \quad (10)$$

where (\Leftarrow Prusa & Smolar. *ibid.*)

$$\psi' := \psi - \psi_e ; \quad \bar{\nabla} := \partial/\partial\bar{\mathbf{x}} ; \quad \tilde{\mathbf{G}} \sim (\partial\bar{\mathbf{x}}/\partial\mathbf{x})$$

$$d/d\bar{t} = \partial/\partial\bar{t} + \bar{\mathbf{v}}^* \bullet \bar{\nabla} ; \quad \bar{\mathbf{v}}^* := d\bar{\mathbf{x}}/d\bar{t} := \dot{\bar{\mathbf{x}}}$$

$$\bar{\mathbf{v}}^s \equiv \bar{\mathbf{v}}^* - \frac{\partial\bar{\mathbf{x}}}{\partial t} ; \quad \bar{\mathbf{v}}^s = \tilde{\mathbf{G}}^T \mathbf{v} . \quad (11)$$

Finite-Difference Approximations

◦ Smolar. & Prusa, *Turbulent Flow Computation*, Kluwer, 2002

• Each prognostic equation can be written as a *Lagrangian* evolution equation or *Eulerian* conservation law:

$$\frac{d\psi}{dt} = R \Leftrightarrow \frac{\partial \rho^* \psi}{\partial t} + \nabla \bullet (\rho^* \mathbf{v}^* \psi) = \rho^* R, \quad (12)$$

Where, $\rho^* := \rho_b \bar{G}$, $\psi \equiv v^j$ or θ , and R the associated rhs.

• Either form is approximated to $\mathcal{O}(\delta t^2, \delta x^2)$ with

$$\psi_{\mathbf{i}}^{n+1} = LE_{\mathbf{i}}(\psi^n + 0.5\delta t R^n) + 0.5\delta t R_{\mathbf{i}}^{n+1} := \widehat{\psi} + 0.5\delta t R_{\mathbf{i}}^{n+1}, \quad (13)$$

where $\psi_{\mathbf{i}}^{n+1}$ is the solution sought at the grid point $(\bar{t}^{n+1}, \bar{\mathbf{x}}_{\mathbf{i}})$, LE denotes a two-time-level either advective semi-Lagrangian or flux-form Eulerian NFT transport operator (viz. advection scheme).

Elliptic Pressure Equation: *exact projection*

• The algorithm in (13) forms system *implicit* for all ψ (v^j , θ') because all (principal) R^{n+1} are unknown \Rightarrow

$$\mathbf{v}_i = \widehat{\mathbf{v}}_i - 0.5\Delta t(\widetilde{\mathbf{G}}(\nabla\pi'))_i + 0.5\Delta t\mathbf{R}_i(\mathbf{v}, \widehat{\theta}), \quad (14)$$

where

$$\mathbf{R}_i(\mathbf{v}, \widehat{\theta}) \equiv -(\mathbf{f} \times (\mathbf{v} - \mathbf{v}_e))_i - \mathbf{g} \frac{1}{\theta_b} (\widehat{\theta}_i + 0.5\Delta t((\widetilde{\mathbf{G}}^T \mathbf{v}) \bullet \nabla\theta_e)_i) \quad (15)$$

accounts for the implicit representation of the buoyancy via (10).

• On grids unstaggered for ψ (e.g., A or B), (14) can be inverted algebraically to construct expressions for $\bar{\mathbf{v}}^s$ via (11) that, after substitution to (8), produce BVP implied by the model discretization:

$$\left\{ \frac{\Delta t}{\rho^*} \nabla \cdot \rho^* \widetilde{\mathbf{G}}^T [\widehat{\mathbf{v}} - (\mathbf{I} - 0.5\Delta t\mathbf{R})^{-1} \widetilde{\mathbf{G}}(\nabla\pi'')] \right\}_i = 0; \quad (16)$$

$\widehat{\mathbf{v}} - (\mathbf{I} - 0.5\Delta t\mathbf{R})^{-1} \widetilde{\mathbf{G}}(\nabla\pi'') \equiv \bar{\mathbf{v}}^s$ defined in (11), and $\pi'' := 0.5\delta t\pi'$.

• Boundary conditions imposed on $\bar{\mathbf{v}}^s \bullet \bar{\mathbf{n}}$, subject to the integrability condition $\int_{\partial\mathcal{S}_t} \rho^* \bar{\mathbf{v}}^s \bullet \bar{\mathbf{n}} d\sigma = 0$, constrain $\nabla\pi''$.

• The resulting BVP is solved using a preconditioned GCR(k) solver. Given updated π'' , and hence the updated $\bar{\mathbf{v}}^s$, the updated \mathbf{v} and \mathbf{v}^* are constructed from $\bar{\mathbf{v}}^s$ using transformations in (11).

RESULTS

- Flapping membranes (Wedi & Sm., *JCP*, **193** 2004):

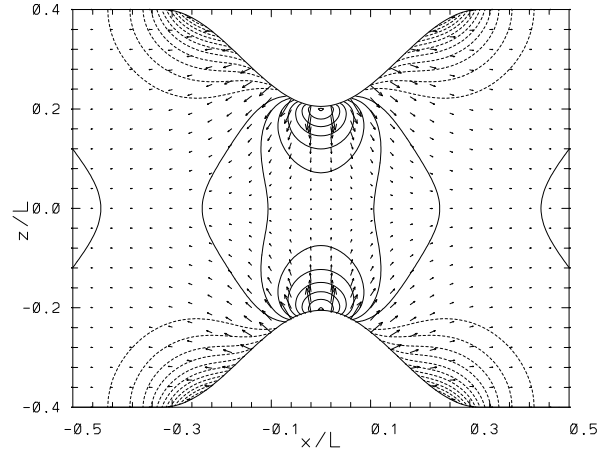


Figure 3: Potential flow simulation past 3D undulating boundaries

semi-Lagrangian model option; $152 \times 152 \times 121$ grid;
 $T = 48\delta t$; $\mathcal{C} \approx 5$, $\mathcal{L} \approx 0.5$; GCR(4)
 Dirichlet boundaries for \mathbf{v} ; 16 PE of IBM SP RS/6000.

For $\| (\delta t / \rho^*) \bar{\nabla} \cdot \rho^* \bar{\mathbf{v}}^s \|_{\infty} < 10^{-5} \Rightarrow$

SP: $\overline{NI}^{22\delta t} = 17$, wallclock time 0:18:16

LR: $\overline{NI}^{22\delta t} = 105$, wallclock time 0:42:24

Table 1: Vorticity errors

field	Max ·	Average	Std. dev.
$\frac{\delta t}{\overline{G}} \bar{\nabla} \cdot \overline{G} (\tilde{\mathbf{G}}^T \boldsymbol{\omega})$	$2.94 \cdot 10^{-5}$	$-7.52 \cdot 10^{-18}$	$3.75 \cdot 10^{-7}$

- Decaying turbulence in a triply periodic box (Herring & Kerr, *Phys. Fluids A*, **5**, 1993; Margolin et al., *J. Fluid Eng.*, **124** 2002):

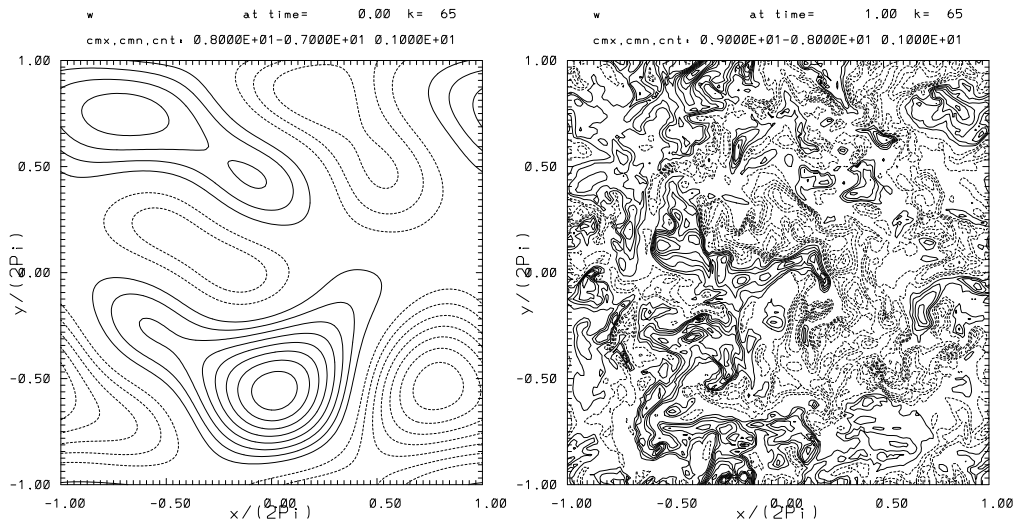


Figure 4: Decaying turbulence

Eulerian model option; Statistics after $10\delta t$; $\delta t \|\nabla \cdot \mathbf{v}\|_{\infty} < 10^{-7}$

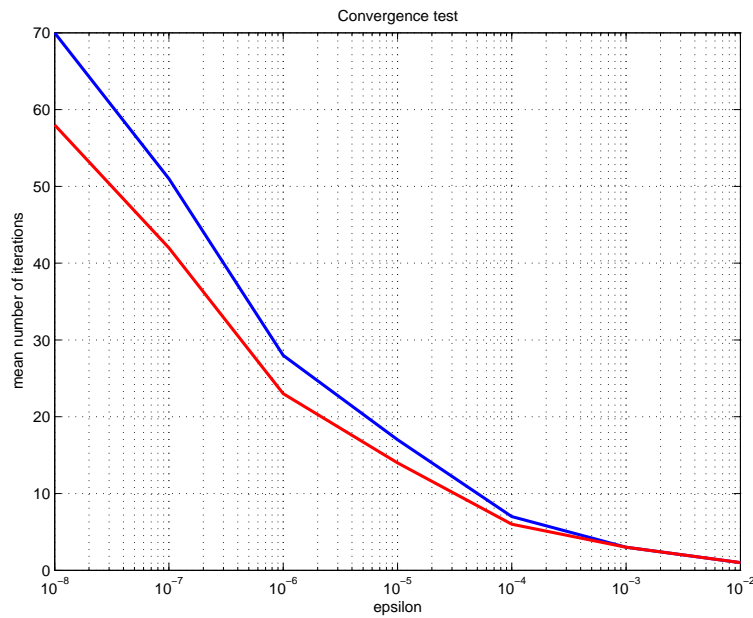


Figure 5: GCR(2) iterations required for the convergence

Table 2: Relative cost of the SP components

PE	FT	3dg-solv.	FT ⁻¹
1	17.36	4.63	18.62
4	2.37	1.04	2.23
8	1.38	0.43	1.08
16	1.04	0.17	0.63
32	1.33	0.06	0.76
64	1.79	0.03	0.59

Table 3: Parallel performance of LR and SP preconditioners; 128³ grid

PE	PX	PY	X1Y1	X1Y0	X0Y1	X0Y0	X1Y1	X1Y0	X0Y1	X0Y0
1	1	1	4650	7920	7535	10659	591	519	459	503
4	2	2	648	-	-	-	123	115	111	79
8	2	4	336	-	-	-	93	61	53	45
8	4	2	348	-	-	-	121	57	62	46
16	4	4	214	-	-	-	54	36	32	28
32	4	8	163	-	-	-	40	29	25	29
32	8	4	179	-	-	-	45	29	28	25
64	8	8	92	-	-	-	47	44	34	36

Table 4: Parallel performance of LR and SP preconditioners; 256³ grid

PE	PX	PY	X1Y1	X1Y1	X0Y0
64	8	8	1553	380	252
128	16	8	961	350	212
256	16	16	529	358	212

♡ Regardless of poorer scaling, SP wins big ♡

• Mesoscale valley flows (cf. Prusa & Smolar. *ibid.*):

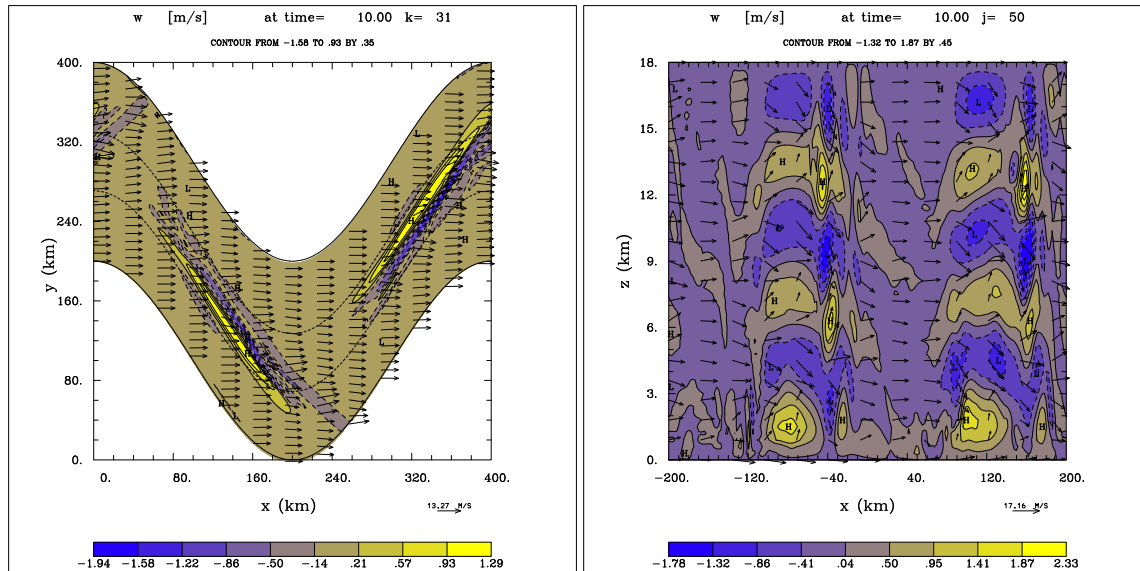


Figure 6: Valley flow. Vertical velocity contours in xy cross section at $z=9$ km (left) and on the vertical ribbon aligned with the center of the valley (right).

Eulerian model option; $200 \times 100 \times 61$ grid;
 $NT = 1200$, $C_{\sim} < 1$; IBM SP RS/6000.

For $\| (\delta t / \rho^*) \bar{\nabla} \cdot \rho^* \bar{\mathbf{v}}^s \|_{\infty} < 10^{-5} \Rightarrow$

SP: $\overline{NI}^{1200\delta t} = 4$, wallclock time 2:54:33, 20 PE

LR: $\overline{NI}^{1200\delta t} = 10$, wallclock time 1:42:24, 20 PE

For $\| (\delta t / \rho^*) \bar{\nabla} \cdot \rho^* \bar{\mathbf{v}}^s \|_{\infty} < 10^{-7} \Rightarrow$

SP: $\overline{NI}^{1200\delta t} = 13$, wallclock time 4:46:21, 40 PE

LR: $\overline{NI}^{1200\delta t} = 87$, wallclock time 2:42:02, 40 PE

- Held-Suarez climate simulations (Sm. et al. *JAS*, **58** 2001):

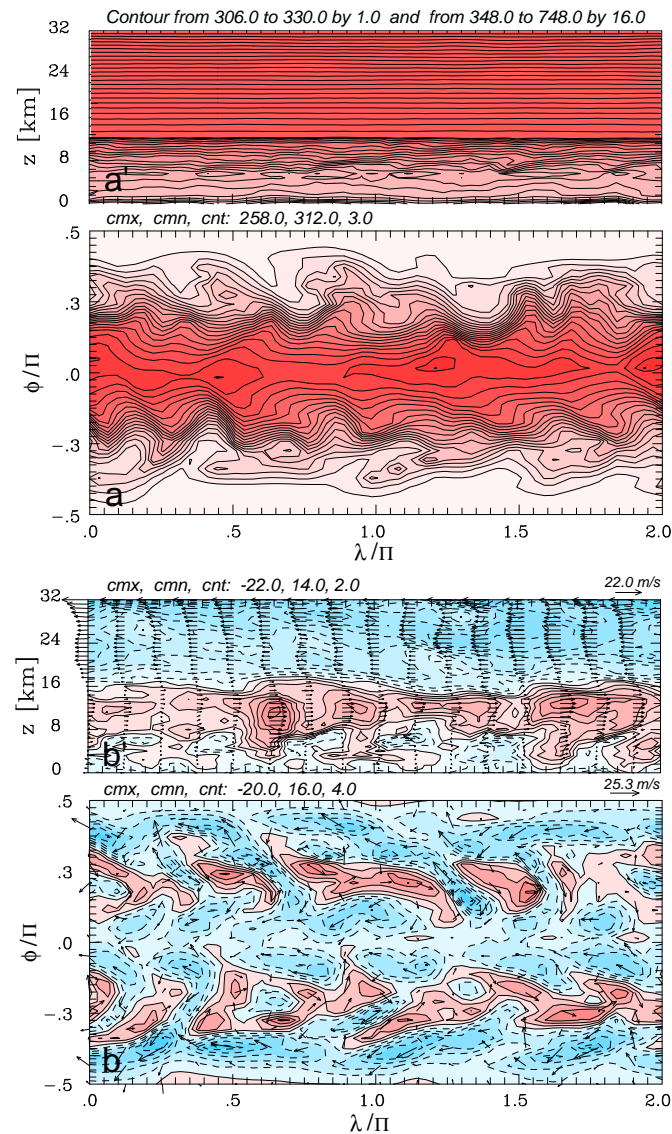


Figure 7: Instantaneous solutions of the idealized climate problem after 3 years of simulation.

Eulerian model option; $66 \times 32 \times 41$ geospherical grid;
 $NT = 2304$, $\mathcal{C} \lesssim 0.5$; 24 PE of IBM SP RS/6000.

For $\| (\delta t / \rho^*) \bar{\nabla} \cdot \rho^* \bar{\mathbf{v}}^s \|_\infty < 10^{-5} \Rightarrow$

SP: Total failure, no convergence in the GCR!

LR: $\overline{NI}^{2304\delta t} = 11$, wallclock time 0:25:04

The observed failure of spectrally-preconditioned GCR is not unique to large scale flows.

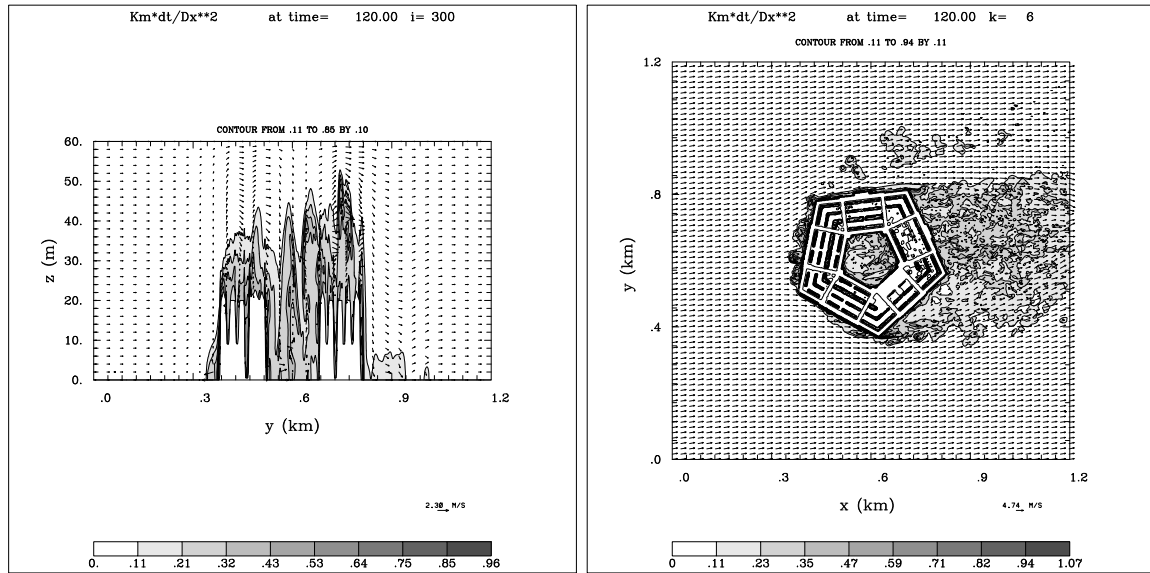


Figure 8: Urban PBL; \sqrt{TKE} contours in xy cross section at $z=10$ m (left) and in the central yz cross section (right).

Eulerian model option; $600 \times 600 \times 31$ grid;
 $NT = 3 \times 2404$, $\mathcal{C} \lesssim 0.8$; IBM SP RS/6000.

For $\| (\delta t / \rho^*) \bar{\nabla} \cdot \rho^* \bar{\mathbf{v}}^s \|_\infty < 10^{-5} \Rightarrow$

SP: 64 PE, $\overline{NI}^{30\delta t} = 56$, wallclock time 3:32:18

LR: 200 PE, $\overline{NI}^{2400\delta t} = 10$, wallclock time 3:55:57

REMARKS

- SP preconditioners are a useful option, but not a panacea. In particular, the *coefficient homogenization* appears destructive for the solver convergence in problems with substantial variability of the coefficients in the horizontal.

- Depending upon the problem at hand, simpler LR preconditioners can be much more effective than SP.

- Since SP preconditioners have substantial overhead compared to LR, it appears counterproductive to use them in problems where the main solver converges in several iterations with LR. Conversely, SP may be advantageous in large-time-step integrations where LR require numerous iterations of the main solver, or where $\mathcal{SP} = \mathcal{L}$.

- SP preconditioners may win big in inherently transient problems, where LR cannot take advantage from slow variability (and thus additivity with solver iterations) of the solution in a portion of the spectral range.

- MPP programing effort can be substantial